

# On the Most Typical Structure of Three-Dimensional Magnetic Reconnection

Yu. V. Dumin<sup>1,2\*</sup> and B. V. Somov<sup>1\*\*</sup>

<sup>1</sup>*Sternberg Astronomical Institute,  
Moscow State University, Universitetskii pr. 13, Moscow, 119992 Russia*

<sup>2</sup>*Space Research Institute, Russian Academy of Sciences, Profsoyuznaya ul. 84/32, Moscow, 117997 Russia*

Received May 10, 2016

**Abstract**—Motivated by the problem of magnetic reconnection in turbulent astrophysical plasmas with a strong magnetic field, in particular, in solar flares, we have calculated the probability of occurrence of various topological structures of three-dimensional reconnection at the null point of a random magnetic field. We have established that the peculiar nonaxisymmetric structure with six asymptotic directions, the six-tailed structure, also called the improper radial null, plays a dominant role. All the remaining structures, in particular, the axisymmetric ones (the proper radial nulls), occur with a much lower probability. The fundamental feature of the six-tailed structure is that at large distances it is approximately reduced to the classical two-dimensional X-type structure.

**DOI:** 10.1134/S1063773716110037

Keywords: *magnetic fields, magnetic reconnection, magnetic field topology.*

## INTRODUCTION

The redistribution of magnetic fluxes (magnetic reconnection), which changes the topological connectivity of magnetic field lines (see, e.g., Priest and Forbes 2005; Somov 2013; and references therein), is currently believed to be responsible for the dynamical character of various astrophysical objects, from the planetary magnetospheres to the intergalactic medium. Magnetic reconnection plays a key role in the laboratory and numerical simulations of flare-type phenomena in astrophysical plasmas (Gonzalez and Parker 2016; Frank et al. 2011).

Magnetic fields often form complex systems containing many places (points or lines) where reconnection can occur. According to Parker (1988), the solar corona is heated as a result of multiple reconnection events in a system that consists of a large number of densely packed magnetic flux tubes. Reconnecting current layers are formed in the places of interaction between these flux tubes; “nanoflares” occur that heat the solar corona. A similar example of complex magnetic systems is the “spaghetti” model of solar flares suggested by de Jager (1986). Subsequently, the model was renamed the “avalanche” model of flares, because it implies that the release of energy in a flare can be understood as a magnetohydrodynamic

(MHD) turbulent cascade (Lu and Hamilton 1991). Turbulence in plasmas with strong magnetic fields (Iroshnikov 1964; Kraichnan 1965) is peculiar to the applications we consider. Studying the peculiarities of reconnection in complex magnetic systems is a topical problem in modern astrophysics, especially in the physics of turbulent space plasmas (Lazarian 2014; Fleishman and Toptygin 2013).

The electric currents in plasmas are always pinched, i.e., they tend to more concentrated states. The pinched current layers are such states in laminar plasmas with strong magnetic fields (Syrovatskii 1981). This property of currents is especially conspicuous in MHD turbulent plasmas. The current configurations are self-organized and structured; they dissipate and regenerate, thereby determining the dissipative and transport properties of turbulent plasmas. In a turbulent plasma with a strong magnetic field the multiple filaments (and layers) with concentrated currents are separated by strong magnetic fields, which can have numerous null points because of their complexity. To understand the dynamical and dissipative properties of such plasmas, it is important to know the topological properties of the magnetic field or, more specifically, the presence of nulls of various types and the probability of occurrence of a particular type.

Recall that the classical approach to studying the magnetic reconnection effect suggests its develop-

\*E-mail: [dumin@yahoo.com](mailto:dumin@yahoo.com)

\*\*E-mail: [somov.boris@gmail.com](mailto:somov.boris@gmail.com)

ment from the null point where all components of the magnetic field vector  $\mathbf{B}$  disappear, thereby violating the condition of field “freezing” into the plasma. Historically, the studies of reconnection began with the simplest two-dimensional (2D) models, where the null points form a straight line and the magnetic field has an X-type structure. However, beginning from the 1980s (Gorbachev et al. 1988; Gorbachev and Somov 1989), the interest in three-dimensional (3D) reconnection, where more diverse topological structures are admissible, has increased rapidly (see the reviews by Pontin (2011) and Somov (2008)).

If the magnetic field is strong (see, e.g., Somov 2013, Ch. 2), then, to a first approximation, it may be considered outside the field sources, i.e., the currents, as a potential magnetic field. Varying in time in accordance with the boundary conditions, the magnetic field reconnects at the null points, i.e., a redistribution of magnetic fluxes occurs, which changes the topological connectivity of the field lines. The structure of the potential field in the vicinity of a 3D null point plays a crucial role and can be pictorially presented as the “collision” of two oppositely directed magnetic fluxes followed by their spreading in the “equatorial” plane. Such spreading (“fan”) can be both axisymmetric (which is called “the proper radial null” in the terminology of Parnell et al. (1996)) and nonaxisymmetric (which is called accordingly “the improper radial null”).

It was implicitly assumed in most of the previously published works that the axisymmetric fan-type structure (proper radial null) was the most typical case of a 3D null point and it could serve as a good initial approximation in 3D reconnection problems. On the other hand, numerical simulations of magnetic fields whose initial structures were significantly non-axisymmetric (improper radial nulls) were undertaken in several papers devoted to the discussion of “typical” 3D reconnection (Al-Hachami and Pontin 2010; Galsgaard and Pontin 2011; Pontin et al. 2011). Unfortunately, it remained unclear how important such structures are from a statistical point of view, in other words, how often they appear in a random magnetic field. The goal of this paper is to carefully calculate the corresponding probabilities. Thus, it will be possible to formulate well-founded criteria for choosing the initial magnetic field structures in the studies of 3D reconnection.

## FORMULATION OF THE PROBLEM AND ITS SOLUTION

### Previous Studies

A universally accepted method of analyzing the structure of the magnetic field  $\mathbf{B}$  in the vicinity of a null point is its Taylor expansion in a Cartesian

coordinate system  $\mathbf{x} = (x_1, x_2, x_3)$  with the origin at the null point:

$$B_i = \sum_{j=1}^3 M_{ij}x_j + \dots, \tag{1}$$

where  $M_{ij} = \left. \frac{\partial B_i}{\partial x_j} \right|_{\mathbf{x}=0}$

(Gorbachev et al. 1988; Parnell et al. 1996; Somov 2008). Since the magnetic field satisfies the Maxwell equations, the elements of the matrix  $\mathbf{M}$  are not independent. Generally (in the presence of electric currents), this matrix can be reduced to four independent parameters (see Eq. (14) in Parnell et al. (1996)).

It is quite obvious that the greater the number of employed (free) parameters and the domain of their admissible values, the higher the probability of occurrence of the corresponding field structures. However, it is very difficult to prove this assumption using Eq. (1), because the elements of the matrix  $\mathbf{M}$  are related to one another and it is not clear how their joint probability distributions should be chosen in parameterizing a random magnetic field.

One way to circumvent this difficulty is to use an explicit solution (for example, in terms of spherical functions), because the corresponding expansion coefficients can be chosen as independent random variables. Here, this procedure will be implemented for a potential magnetic field (without electric currents within the neighborhood of the null point under consideration). A similar analysis for a nonpotential magnetic field involves much more cumbersome mathematics and is beyond the scope of this paper.

### Initial Equations

We will consider the *random realizations* of a potential magnetic field

$$\mathbf{B} = -\text{grad}\psi, \tag{2}$$

where the potential  $\psi$  satisfies the Laplace equation

$$\Delta\psi = 0. \tag{3}$$

Assuming that the null point is located at the origin of a spherical coordinate system  $(r, \theta, \varphi)$ , the solution of Eq. (3) can be written in a standard way as

$$\psi(r, \theta, \varphi) = \sum_{j=0}^{\infty} \sum_{m=0}^j r^j \psi_{jm}(\theta, \varphi), \tag{4}$$

where

$$\begin{aligned} & \psi_{jm}(\theta, \varphi) \\ &= P_j^m(\cos\theta) [a_{jm} \cos(m\varphi) + b_{jm} \sin(m\varphi)] \end{aligned} \tag{5}$$

are the spherical functions, and  $P_j^m$  are the adjoint Legendre polynomials. The terms with negative powers of  $r$  are not written out here, because we are interested in the solutions that do not become infinite at zero. In addition, to avoid considering infinite sums, we will assume that Eq. (4) is cut off at some sufficiently large value of  $j$ , i.e., it contains only a finite number of terms  $N$ . In other words,  $N$  is the dimensionality of the space of coefficients  $a_{jm}$  and  $b_{jm}$ .

If the above coefficients are specified by random numbers, then we get some random realization of the magnetic field  $\mathbf{B}$ . The question of how to choose the adequate probability distributions for each coefficient requires a separate consideration. However, we will emphasize that most of our conclusions will be based only on the dimensionality of various subsets of coefficients  $a_{jm}$  and  $b_{jm}$  related to various types of reconnection. Thus, the corresponding results must be valid for any nonsingular probability distribution.

Let us analyze the terms of potential (4) with various powers of  $r$ . At  $j = 0$  we have

$$\psi^{(0)} = a_{00} = \text{const}, \quad (6)$$

which obviously does not affect any physical results.

Next, at  $j = 1$  the potential is

$$\psi^{(1)} = r \left\{ a_{10} \cos \theta - (1 - \cos^2 \theta)^{1/2} [a_{11} \cos \varphi + b_{11} \sin \varphi] \right\}, \quad (7)$$

and its substitution into (2) leads to

$$B_r^{(1)} = - \left\{ a_{10} \cos \theta - (1 - \cos^2 \theta)^{1/2} [a_{11} \cos \varphi + b_{11} \sin \varphi] \right\}. \quad (8)$$

Since  $r = 0$  is a null point (i.e., all magnetic field components, including  $B_r$ , disappear), we arrive at the condition

$$a_{10} = a_{11} = b_{11} = 0. \quad (9)$$

In view of these three constraints, a null point of any type is realized in the subspace of random coefficients  $a_{jm}$  and  $b_{jm}$  with dimensionality  $N - 3$  or less.

At  $j = 2$  the potential is written as

$$\psi^{(2)} = r^2 \left\{ \frac{1}{2} (3 \cos^2 \theta - 1) a_{20} - 3 \sin \theta \cos \theta [a_{21} \cos \varphi + b_{21} \sin \varphi] + 3 \sin^2 \theta [a_{22} \cos 2\varphi + b_{22} \sin 2\varphi] \right\}. \quad (10)$$

Since we are interested in the structure of the magnetic field lines and not in its absolute values, it is convenient to introduce normalized coefficients denoted by a single subscript:

$$a_m = a_{2m}/a_{20}, \quad b_m = b_{2m}/a_{20}, \quad m = 1, 2. \quad (11)$$

The field components will then be

$$B_r^{(2)} = -2a_{20}r \left\{ \frac{1}{2} (3 \cos^2 \theta - 1) - \frac{3}{2} \sin 2\theta [a_1 \cos \varphi + b_1 \sin \varphi] + 3 \sin^2 \theta [a_2 \cos 2\varphi + b_2 \sin 2\varphi] \right\}, \quad (12a)$$

$$B_\theta^{(2)} = -3a_{20}r \left\{ \sin 2\theta \left[ -\frac{1}{2} + a_2 \cos 2\varphi + b_2 \sin 2\varphi \right] - \cos 2\theta [a_1 \cos \varphi + b_1 \sin \varphi] \right\}, \quad (12b)$$

$$B_\varphi^{(2)} = -3a_{20}r \left\{ 2 \sin \theta \left[ -a_2 \sin 2\varphi + b_2 \cos 2\varphi \right] + \cos \theta [a_1 \sin \varphi - b_1 \cos \varphi] \right\}. \quad (12c)$$

### Asymptotic Directions

Following the standard technique, we will write the equation for a magnetic field line as

$$\frac{dr}{B_r/(a_{20}r)} = \frac{rd\theta}{B_\theta/(a_{20}r)} = \frac{r \sin \theta d\varphi}{B_\varphi/(a_{20}r)}. \quad (13)$$

Since the quantities  $B_r^{(2)}/(a_{20}r)$ ,  $B_\theta^{(2)}/(a_{20}r)$ , and  $B_\varphi^{(2)}/(a_{20}r)$  do not depend on  $r$ , passing to the limit  $r \rightarrow 0$  we obtain the conditions specifying the field lines that pass directly through the null point:

$$B_\theta^{(2)}/(a_{20}r) = 0, \quad B_\varphi^{(2)}/(a_{20}r) = 0. \quad (14)$$

Substituting (12b) and (12c) into (14) gives the following system of algebraic equations:

$$\sin 2\theta^* \left[ -\frac{1}{2} + a_2 \cos 2\varphi^* + b_2 \sin 2\varphi^* \right] - \cos 2\theta^* [a_1 \cos \varphi^* + b_1 \sin \varphi^*] = 0, \quad (15a)$$

$$2 \sin \theta^* [-a_2 \sin 2\varphi^* + b_2 \cos 2\varphi^*] + \cos \theta^* [a_1 \sin \varphi^* - b_1 \cos \varphi^*] = 0, \quad (15b)$$

where  $\theta^*$  and  $\varphi^*$  are the angles at which the corresponding field lines enter or leave the null point.

It is easy to check that the system of equations (15a) and (15b) is invariant with respect to the transformation:  $\theta^* \rightarrow \pi - \theta^*$ ,  $\varphi^* \rightarrow \varphi^* + \pi$ . Consequently, the magnetic field lines passing through the null point always appear as sets of oppositely directed pairs. Thus, the geometric structures with an odd

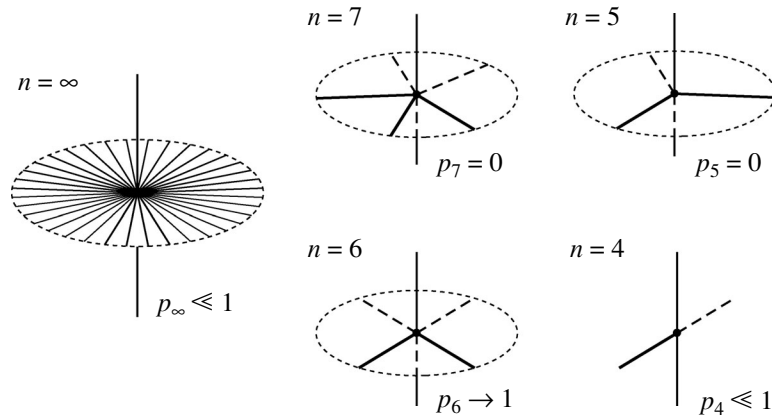


Fig. 1. Scheme of several hypothetical null points, including both the axisymmetric fan structure (left) and the structures with a finite number of asymptotic directions  $n$  (right).

number of tails (for example,  $n = 5$  or  $7$  in Fig. 1) cannot exist at all.

Let us analyze some particular solutions of Eqs. (15a) and (15b). The simplest case obviously takes place at  $a_1 = b_1 = a_2 = b_2 = 0$  or, in the original notation,

$$a_{2m} = 0, b_{2m} = 0, \quad \text{where } m = 1, 2. \quad (16)$$

Our equations are then reduced to the simple condition

$$\sin 2\theta^* = 0, \quad (17)$$

which has a solution of two types:

$$\theta^* = 0, \pi, \quad (18a)$$

$$\theta^* = \pi/2 \quad \text{at any } \varphi^*. \quad (18b)$$

This solution is a combination of the polar axis and disk in the equatorial plane, i.e., precisely the axisymmetric fan structure depicted in the left part of Fig. 1. It was called the “proper radial null” by Parnell et al. (1996), and this term was subsequently used by other authors.

In view of the four additional constraints (16), at first glance it seems that such a structure will be realized in the subspace of coefficients  $a_{jm}$  and  $b_{jm}$  with dimensionality  $N - 3 - 4 = N - 7$ . However, recall that these constraints were formulated for the peculiar situation where the fan axis was oriented along the polar axis of the spherical coordinate system. In general, this structure can be rotated in space through two Euler angles, which actually removes two constraints. Thus, the dimensionality of the corresponding subset of coefficients must be  $N - 7 + 2 = N - 5$ .

Returning to the general case of arbitrary coefficients  $a_1, b_1, a_2,$  and  $b_2$ , it is natural to expect that the system of two algebraic equations (15a) and (15b) for the two unknown variables  $\theta^*$  and  $\varphi^*$  must have some

finite number of solutions, i.e., the number of asymptotic tails in Fig. 1 must be finite. Moreover, as follows from a more careful analysis, this number is always equal to six, if some special subset of coefficients  $a_i$  and  $b_i$  with lower dimensionality is disregarded.

To prove this assertion, it is convenient to reduce the system of equations (15a) and (15b) to one equation for the azimuthal angle  $\varphi^*$ :

$$F(\eta(\varphi^*), \zeta(\varphi^*)) = 0, \quad (19)$$

where  $\eta = \cos \varphi^*, \zeta = \sin \varphi^*$ , and

$$F(\eta, \zeta) = 4[2a_2\eta\zeta - b_2(\eta^2 - \zeta^2)](a_1\zeta - b_1\eta) \times \left[ -\frac{1}{2} + a_2(\eta^2 - \zeta^2) + 2b_2\eta\zeta \right] - \left\{ 4[2a_2\eta\zeta - b_2(\eta^2 - \zeta^2)]^2 - (a_1\zeta - b_1\eta)^2 \right\} \times (a_1\eta + b_1\zeta). \quad (20)$$

Once the roots  $\varphi^*$  have been found, the corresponding values of the polar angle  $\theta^*$  can be easily restored from one of Eqs. (15a) or (15b).

Since Eq. (20) is a very complex polynomial expression, the simplest method of solving our problem is to perform statistical simulations, i.e., to generate a sufficiently large sequence of random coefficients  $a_1, a_2, b_1,$  and  $b_2$  (for example, in the form of a Gaussian distribution with zero mean) and then to analyze the behavior of the function  $F(\eta(\varphi^*), \zeta(\varphi^*))$  graphically (Fig. 2). As a result, quite an unexpected property is established: the plot of  $F$  always intersects the horizontal axis exactly at three points in the interval  $\varphi^* \in [0, \pi]$  (and, consequently, at six points in the interval  $\varphi^* \in [0, 2\pi]$ ). A subsequent more careful analysis allowed us to obtain a rigorous mathematical proof of this fact. However, in view of the cumbersome formulas, we prefer not to discuss it here but to appeal just to the results of our statistical simulations.

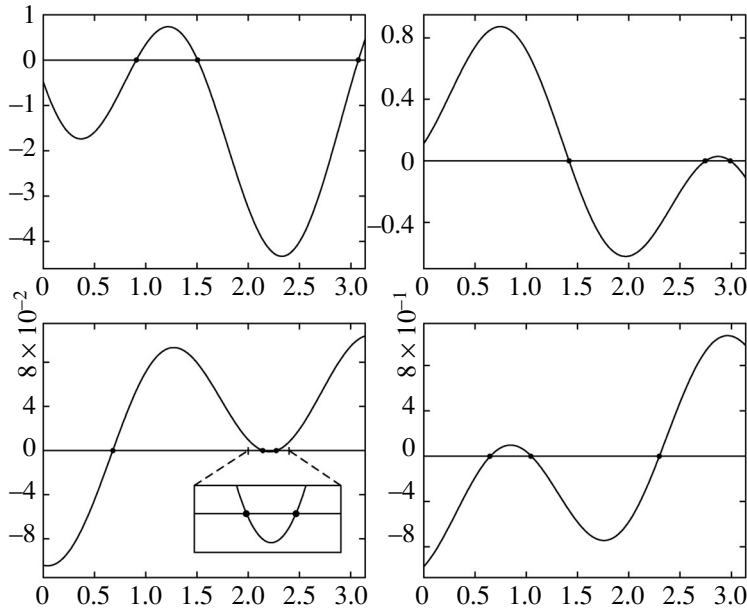


**Fig. 2.** Examples of the function  $F(\eta(\varphi^*), \zeta(\varphi^*))$  in the interval  $\varphi^* \in [0, \pi]$  at random values of the coefficients  $a_1$ ,  $a_2$ ,  $b_1$ , and  $b_2$ .

Furthermore, it can be shown that six solutions of Eqs. (15a) and (15b) geometrically correspond to six tails mutually orthogonal to one another.

Thus, we established that the generic 3D null point in the potential field approximation has a six-tailed structure, i.e., it possesses six asymptotic directions of the magnetic field. Such a null point is typical, because it is realized in the subset of coefficients of a random field with dimensionality  $N - 3$ , i.e., almost everywhere where the null point can emerge according to the constraints (9). All the remaining structures (in particular, the axisymmetric fan as well as more exotic structures mentioned by Zhugzhda (1966)) must emerge with much lower probabilities, because they are realized in the subsets of coefficients with lower dimensionality. We will emphasize that all these conclusions are based only on the reasoning about the dimensionality of the corresponding subspaces and, therefore, they are valid for any nonsingular probability distribution of the random-field coefficients. The specific distribution that we used in our simulations presented in Fig. 2 does not affect the final result.

### *The Structure of Magnetic Field Lines*

Consider the overall pattern of magnetic field lines in the vicinity of the “typical” null point found above. The simplest (but without any loss of generality) case of  $a_1 = b_1 = b_2 = 0$  and  $a_2 \neq 0$  corresponds to a six-tailed structure oriented along the axes of the Cartesian coordinate system. In this case, Eqs. (15a) and

(15b) for the asymptotic directions take a simple form:

$$\sin 2\theta^* \left[ -\frac{1}{2} + a_2 \cos 2\varphi^* \right] = 0, \quad (21a)$$

$$a_2 \sin \theta^* \sin 2\varphi^* = 0, \quad (21b)$$

and their solutions are  $\theta^* = 0, \pi$ , and  $\pi/2$ ,  $\varphi^* = 0, \pi/2, \pi$ , and  $3\pi/2$ , corresponding to six semiaxes of the coordinate system.

Omitting the nonessential common factor  $a_{20}$  in Eqs. (12a)–(12c), we obtain the following expressions for the field components:

$$B_r = -2r \left[ \frac{1}{2}(3\cos^2\theta - 1) + 3a_2 \sin^2\theta \cos 2\varphi \right], \quad (22a)$$

$$B_\theta = -3r \sin 2\theta \left[ -\frac{1}{2} + a_2 \cos 2\varphi \right], \quad (22b)$$

$$B_\varphi = 6a_2 r \sin \theta \sin 2\varphi. \quad (22c)$$

As would be expected,  $B_\theta$  and  $B_\varphi$  are equal to zero on the coordinate axes, while  $B_r$  has opposite signs on different sides from the center.

After the substitution of (22a)–(22c) into Eq. (13) and integration, we obtain the expressions for magnetic field lines in three coordinate planes. For example, in the  $xy$  plane (i.e.,  $\theta = \pi/2$ ) the final result is

$$r = C \left( |\sin \varphi|^{1-1/(6a_2)} |\cos \varphi|^{1+1/(6a_2)} \right)^{-1/2}, \quad (23)$$

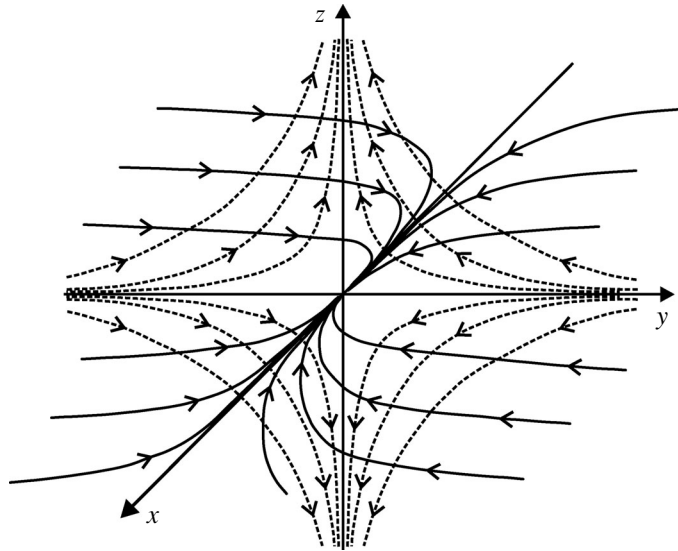


**Fig. 3.** Scheme of magnetic field lines in the vicinity of a six-tailed structure. The solid and dashed curves indicate the field lines in the horizontal  $xy$  and vertical  $yz$  planes, respectively. The field lines in the vertical  $xz$  plane, perpendicular to the plane of the figure, are not shown here; they have the same hyperbolic structure as that in the  $yz$ -plane.

where  $C$  is an arbitrary constant. The behavior of this function has three qualitatively different regimes, depending on the coefficient  $a_2$ :

(a) If  $a_2 < -1/6$  or  $a_2 > 1/6$ , then  $r \rightarrow \infty$  both for  $\varphi \rightarrow 0$  and for  $\varphi \rightarrow \pi/2$ . This corresponds to a hyperbolic magnetic field line.

(b) If  $-1/6 < a_2 < 0$ , then  $r \rightarrow \infty$  for  $\varphi \rightarrow 0$  and  $r \rightarrow 0$  for  $\varphi \rightarrow \pi/2$ . This corresponds to a parabolic field line with the parabola axis oriented in the  $x$  direction.

(c) If  $0 < a_2 < 1/6$ , then  $r \rightarrow 0$  for  $\varphi \rightarrow 0$  and  $r \rightarrow \infty$  for  $\varphi \rightarrow \pi/2$ . This is also a parabolic field line but with the parabola axis oriented in the  $y$  direction.

As regards the magnetic field lines in the two other coordinate planes, they have a hyperbolic structure in cases (b) and (c).

The situation for case (c) is illustrated in Fig. 3. It can be shown that the patterns of magnetic field lines for all the remaining cases can be obtained just by the permutation of coordinate axes. Using the terminology adopted in the theory of differential equations, it can be said that the field lines have a node structure in one of the coordinate planes and a saddle structure in the two other planes.

We will emphasize that the pattern of field lines in the vicinity of a 3D null point in the form of a structure with six asymptotic directions is not new per se: it is known from earlier works (see, for example, Fig. 1 in Gorbachev et al. (1988) or Fig. 5 in Parnell et al. (1996)), where such a structure was called the “improper radial null.” However, strangely enough, it has not been realized until now that precisely this

structure plays a dominant role in 3D magnetic reconnection.

In addition, as follows from an analysis of the literature, many observers were misled by the fact that the term “improper” used by theoreticians actually referred to the situation that is most typical, i.e., it occurs with an overwhelming probability. Therefore, we deemed necessary to introduce a new term for it that reflects its topological nature, a six-tailed structure.

Of course, the purely geometrical properties of this structure can also be studied in Cartesian coordinates using the Taylor expansion (1) (see, for example, Sec. III in Parnell et al. (1996)). The null points of a potential magnetic field were also considered in Cartesian coordinates in connection with the topological trigger effect (see Fig. 9 in Somov (2008)). Meanwhile, our approach based on the expansion in terms of spherical functions provides an additional opportunity, namely, to perform an accurate statistical parametrization of a random magnetic field and, thus, to calculate the corresponding probabilities of occurrence of various topological structures of 3D reconnection at the null point of the random field.

#### *Pictorial Explanation and Discussion of Our Results*

In fact, even from simple considerations it is easy to understand qualitatively why the probability of occurrence of the axisymmetric fan (on the left in Fig. 1) must be strongly suppressed compared to the six-tailed structure. Consider the behavior of the magnetic field lines in the  $xy$  plane (Fig. 3). Suppose that the parameter  $a_2$  initially corresponded to case (c), as

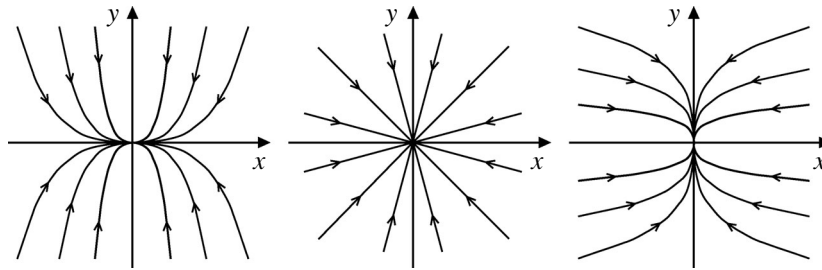


**Fig. 4.** The axisymmetric fan as an intermediate case between the two six-tailed structures. Only the field lines in the  $xy$  plane are displayed here; the field lines in the  $xz$  and  $yz$  planes always remain of the same saddle type.

shown in the left part of Fig. 4. Next, let  $a_2$  gradually decrease and become negative, which corresponds to case (b). Geometrically, this means a gradual decrease in the curvature of the field lines such that at some instant they become straight and then bent in a different direction, i.e., the entire pattern remains parabolic but turns abruptly through  $\pi/2$  (Fig. 4, on the right). The boundary between these two cases at  $a_2 = 0$  precisely corresponds to the axisymmetric fan-type structure shown at the center of the figure.

In other words, there exist infinitely many six-tailed structures of types (b) and (c) but only one intermediate fan-type configuration. That is why the probability of its realization must be extremely low. Note that a similar consideration for a magnetic field parameterized by a different method in Cartesian coordinates was presented in Fig. 2 in Priest and Titov (1996).

Returning to Fig. 3, we will note that the six asymptotic directions of the magnetic field differ greatly from one another in their properties. More specifically, four of them ( $y$ ,  $-y$ ,  $z$ , and  $-z$ ) may be called “dominant,” because most of the field lines tend to approach one of these directions as one recedes from the null point. At the same time, the two other asymptotic directions ( $x$  and  $-x$ ) should be called “recessive,” because most of the field lines recede from them. Thus, the recessive directions will be “lost” when observed from a great distance, and the entire pattern will look like a classical 2D X-point. This fact can explain why the 2D magnetic reconnection models work quite well in many cases. For example, Masson et al. (2009) numerically simulated the solar flare that was presumably triggered by only one null point in the corona and established that the corresponding 3D reconnection actually occurs in quasi-2D slabs.

To avoid misunderstanding, note that the presence of a 3D null point is not always a sufficient condition for the development of reconnection, because this also depends on the efficiency of the accompanying MHD processes or, more precisely, on the presence of an electric field at this point (see Ch. 1 in the book by

Somov (2013)). For example, situations where no appreciable energy release in any form was detected in the solar corona in the presence of a well-defined null point were observed (Filippov 1999). Barnes (2007) comprehensively investigated the relationship between solar eruptive events and the presence of a magnetic null point in the corona using more than 1800 vector magnetograms. Each of them was subjected to a detailed topological analysis based on the method of “magnetic charges” (Gorbachev et al. 1988). It turned out that most events occurred in active regions for which no coronal null points (CNPs) of the magnetic field were found. However, in active regions with CNPs eruptive events occur much more frequently than in active regions where CNPs were absent or not found. More specifically, 73% of all eruptive flares took place in active regions with CNPs. This conclusion is consistent with the results of Ugarte-Urra et al. (2007). The 2D reconnection models often work quite well for explaining the observations, laboratory and numerical simulations of solar flares (see, e.g., Gonzalez and Parker 2016; Frank et al. 2011).

## CONCLUSIONS

Bearing in mind the applications to astrophysical turbulent plasmas with strong magnetic fields, in particular, to magnetic reconnection in solar flares, we calculated the probability of occurrence of various types of 3D null points in a random magnetic field and studied the structure of the field lines in their vicinity. As a result, we established the following:

(1) The most probable case of the 3D null point responsible for triggering magnetic reconnection is the six-tailed magnetic field structure, called the improper radial null in the terminology of Parnell et al. (1996). All the remaining types of 3D null points, in particular, the axisymmetric fan (or the proper radial null) are realized with much lower probabilities, as schematically summarized in Fig. 1.

(2) At sufficiently large distances a typical six-tailed structure is reduced to a quasi-2D structure of

the well-known X-type. This explains why the 2D models often are a good approximation for the description of magnetic reconnection in complex magnetic field configurations. Large-scale manifestations of reconnection in powerful solar flares can be comprehensively studied using modern instruments with a moderate spatial resolution onboard satellites and spacecraft. The 2D reconnection models satisfactorily explain the observations, laboratory and numerical simulations of solar flares.

(3) Based on our results, we can assume that the peculiar 3D magnetic reconnection effects must manifest themselves primarily on sufficiently small scales (for example, in solar micro- and nanoflares), whose observation requires instruments with a very high spatial resolution.

#### ACKNOWLEDGMENTS

We are grateful to the referee for very useful remarks. This study was supported by the Russian Foundation for Basic Research (project no. 16-02-00585 a).

#### REFERENCES

1. A. K. Al-Hachami and D. I. Pontin, *Astron. Astrophys.* **512**, A84 (2010).
2. G. Barnes, *Astrophys. J.* **670**, L53 (2007).
3. B. Filippov, *Solar Phys.* **185**, 297 (1999).
4. G. D. Fleishman and I. N. Toptygin, *Cosmic Electrodynamics: Electrodynamics and Magnetic Hydrodynamics of Cosmic Plasmas* (Springer SBM, New York, 2013).
5. A. G. Frank, N. P. Kyrie, and S. N. Satunin, *Phys. Plasmas* **18**, 111209 (2011).
6. K. Galsgaard and D. I. Pontin, *Astron. Astrophys.* **534**, A2 (2011).
7. W. Gonzalez and E. Parker, *Magnetic Reconnection: Concepts and Applications* (Springer, 2016).
8. V. S. Gorbachev and B. V. Somov, *Sov. Astron.* **33**, 57 (1989).
9. V. S. Gorbachev, S. R. Kel'ner, B. V. Somov, and A. S. Shvarts, *Sov. Astron.* **32**, 308 (1988).
10. P. S. Iroshnikov, *Sov. Astron.* **7**, 566 (1964).
11. C. de Jager, *Space Sci. Rev.* **44**, 43 (1986).
12. R. H. Kraichnan, *Phys. Fluid* **8**, 1385 (1965).
13. A. Lazarian, *Space Sci. Rev.* **181**, 1 (2014).
14. E. T. Lu and R. J. Hamilton, *Astrophys. J.* **380**, L89 (1991).
15. S. Masson, E. Pariat, G. Aulanier, and C. J. Schrijver, *Astrophys. J.* **700**, 559 (2009).
16. E. N. Parker, *Astrophys. J.* **330**, 474 (1988).
17. C. E. Parnell, J. M. Smith, T. Neukirch, and E. R. Priest, *Phys. Plasmas* **3**, 759 (1996).
18. D. I. Pontin, *Adv. Space Res.* **47**, 1508 (2011).
19. D. I. Pontin, A. K. Al-Hachami, and K. Galsgaard, *Astron. Astrophys.* **533**, A78 (2011).
20. E. R. Priest and V. S. Titov, *Phil. Trans. R. Soc. London A* **354**, 2951 (1996).
21. E. Priest and T. Forbes, *Magnetic Reconnection: MHD Theory and Applications* (Cambridge Univ. Press, Cambridge, UK, 2000).
22. B. V. Somov, *Astron. Lett.* **34**, 635 (2008).
23. B. V. Somov, *Plasma Astrophysics, Part II: Reconnection and Flares*, 2nd ed. (Springer SBM, New York, 2013).
24. S. I. Syrovatskii, *Ann. Rev. Astron. Astrophys.* **19**, 163 (1981).
25. I. Ugarte-Urra, H. P. Warren, and A. R. Winebarger, *Astrophys. J.* **662**, 1293 (2007).
26. Yu. D. Zhugzhda, *Geomagn. Aeron.* **6**, 506 (1966).

*Translated by Yu. Dumin*